

MICROBUNCHING INSTABILITY STUDY FOR THE PAL-XFEL LINAC*

J.-H. Han[†], I. Hwang, H.-S. Kang,
 Pohang Accelerator Laboratory (PAL), Pohang, 790-784, Republic of Korea

Abstract

PAL-XFEL is designed to generate X-ray FEL radiation in a range of 0.1 and 10 nm for users. The machine consists of a 10 GeV linear accelerator and five undulator beamlines. An electron beam is generated at a low emittance S-band photoinjector and accelerated through an S-band normal conducting linac. Microbunching instability may occur when the beam goes through magnetic bunch compressors and beam spreaders. We show preliminary microbunching instability simulation study for the PAL-XFEL linac.

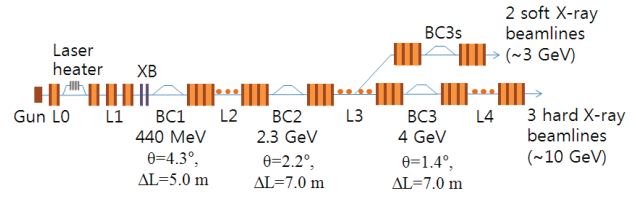


Figure 1: Model layout of the PAL-XFEL linac used for this simulation study.

INTRODUCTION

For the generation of fully coherent hard X-ray laser, the PAL-XFEL linac will deliver a high brightness electron beam from the injector to the undulator beamlines [1]. Small transverse emittance and high peak current of an electron bunch is essential for SASE FEL; however such a high brightness beam may suffer from collective effects. Microbunching instability may impair electron beam quality and make beam image measurements with screen difficult. The PAL-XFEL linac uses three magnetic chicanes for bunch compression for flexible and independent operation of the soft and hard X-ray beamlines [2]. Microbunching may amplify significantly through the chicanes. The linac has a beam branch to the soft X-ray beamlines at the 3 GeV point from the 10 GeV main linac. The branch has a large deflection angle, $3^\circ + 3^\circ$, therefore that is a potential instability source. The electron beam spreaders for three hard and two soft X-ray beamlines are also concerned.

In this preliminary study, the Elegant code [3] is used for beam tracking through the linac including the chicanes. A simplified laser heater model in Elegant is used for simulation including a magnetic chicane, a small undulator and a heat laser. The soft X-ray branch and the beam spreaders are not considered yet in this study.

MODEL LAYOUT

A few model layouts of the linac were studied for beam tracking including microbunching effect. One model showing best electron beam shapes after the linac was chosen for this simulation study. The model layout is shown in Fig. 1.

Beam Tracking with Laser Heater Off

Three initial beam distributions from the injector were used for Elegant tracking simulation: A 200 pC nominal

bunch and a 20 pC low charge bunch from the baseline injector [4] and a 200 pC nominal bunch from the low emittance injector [5]. The simulation result using a 200 pC bunch from the baseline injector is shown in Fig. 2 when heater laser is off. For this simulation, 2M macroparticles was tracked using 200 bins for longitudinal space charge (LSC) and CSR calculation.

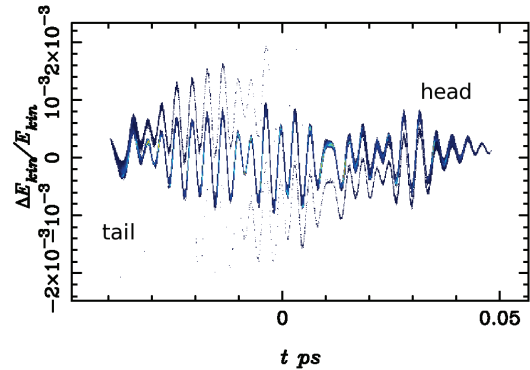


Figure 2: Time-energy phase space at the linac end for a 200 pC beam from the baseline injector. Heater laser is off.

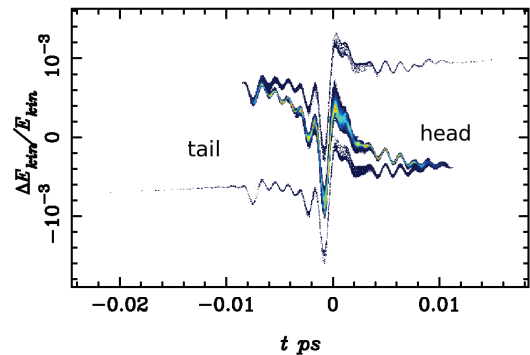


Figure 3: Time-energy phase space at the linac end for a 20 pC beam from the baseline injector. Heater laser is off.

* Work supported by The Ministry of Education, Science and Technology of the Korean Government

[†] janghai.han@postech.ac.kr

A 20 pC bunch from the baseline injector was tracked to generate maximum peak current at the linac end (see Fig.3). A 200 pC bunch from the low emittance injector was tracked with similar conditions as used for 200 pC case (see Fig.4). As shown in the figures, strong microbunching

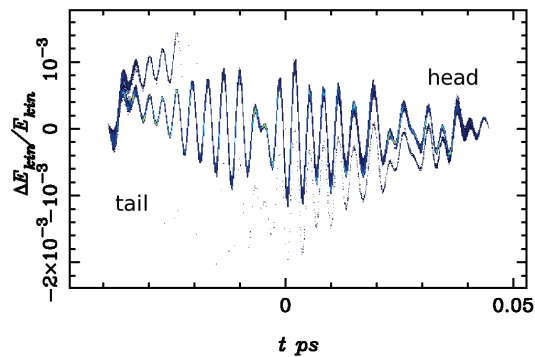


Figure 4: Time-energy phase space at the linac end for a 200 pC beam from the low emittance injector. No heater laser applied.

pattern appears when heater laser is off. In these cases, transverse emittance energy spread become large.

Beam Tracking with Laser Heater On

To minimize such instability, uncorrelated energy spread of a beam may be increased by using a laser heater before the first bunch compressor. The laser heater system designed for the PAL-XFEL linac consists of a magnetic chicane for beam path deflection, a small undulator and a heater laser. The chicane has four 0.1 m long bending magnets. The chicane deflects the beam path by 30 mm from the beam path of the main linac. The undulator has 10 periods with a 50 mm period length. The laser heater effect on 200 pC beams from the baseline injector is shown in Fig. 5.

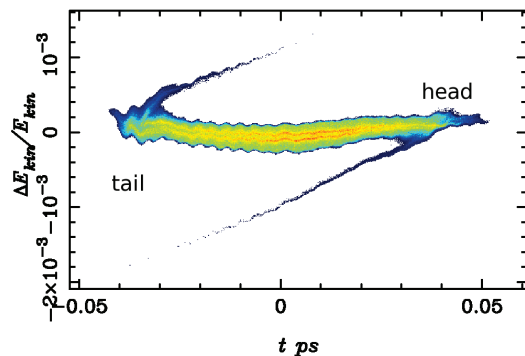


Figure 6: Time-energy phase space at the linac end for a 200 pC beam from the baseline injector. A 60 kW heater laser power was applied to increase the uncorrelated energy spread to 10 keV at the injector end.

For the 200 pC bunch case using the baseline injector, a heater laser power of 60 kW was modeled using the Elegant code in order to increase the uncorrelated energy spread to

ISBN 978-3-95450-123-6

10 keV. The bunch was tracked through the linac and the result is shown in Fig. 6. Such microbunching pattern appeared in Fig. 2 damped down and the uncorrelated energy spread becomes 10^{-4} .

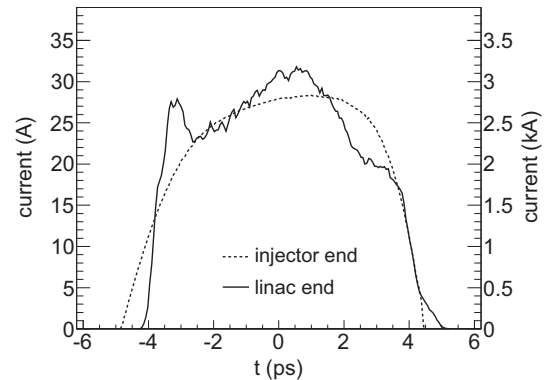


Figure 7: Current distribution of a 200 pC beam at the baseline injector end and at the linac end. The peak current is 26 A at the injector end and 3 kA at the linac end. The time axis for the linac end is multiplied by 100 for the comparison of distribution pattern.

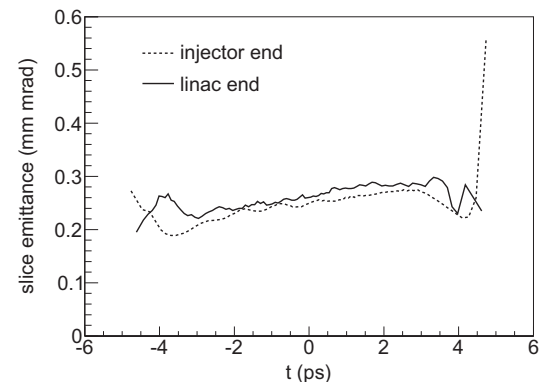


Figure 8: Normalized horizontal slice emittance of a 200 pC beam at the baseline injector and linac ends. The time axis for the linac end is multiplied by 110.

The current profiles of a bunch at the injector and linac ends are compared in Fig. 7 for the 200 pC case from the baseline injector. The normalized horizontal slice emittances are also compared in Fig. 8 at the injector end and at the linac end. Only a little emittance increase is found.

For the 20 pC bunch case from the baseline injector, a heater laser power of 2 kW was applied. The bunch was tracked through the linac and the result is shown in Fig. 9. The current profiles of a bunch at the injector and linac ends are compared in Fig. 10 for the 20 pC case from the baseline injector. The normalized horizontal slice emittances are also compared in Fig. 11 at the injector and linac ends.

For the 200 pC bunch case from the low emittance injector, a heater laser power of 100 kW was applied in order to increase the uncorrelated energy spread to 10 keV. The bunch was tracked through the linac and the result is

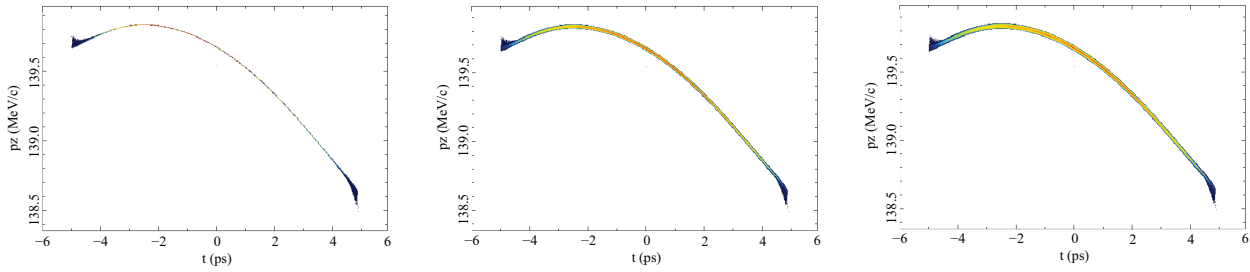


Figure 5: Laser heater effect on beams at the injector end: 0 kW heater laser (left), 40 kW (middle) and 80 kW (right) are applied in Elegant simulation.

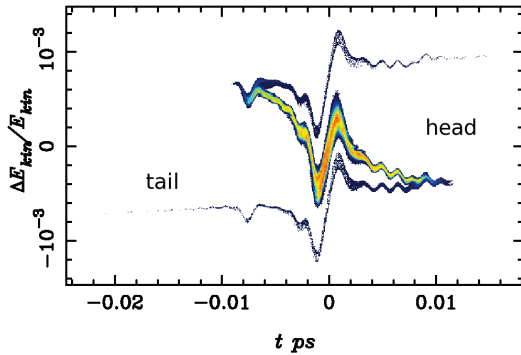


Figure 9: Time-energy phase space at the linac end for a 20 pC beam from the baseline injector. A 2 kW heater laser power was applied.

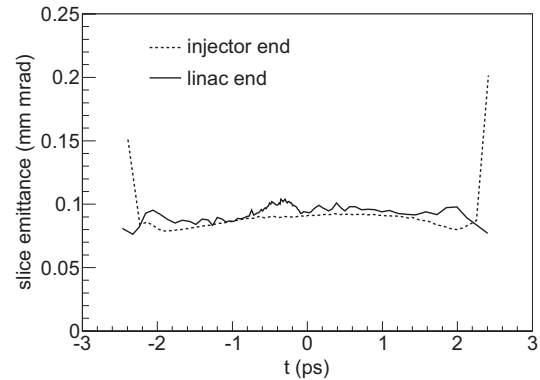


Figure 11: Normalized horizontal slice emittance of a 20 pC beam at the baseline injector and linac ends. The time axis for the linac end is multiplied by 280.

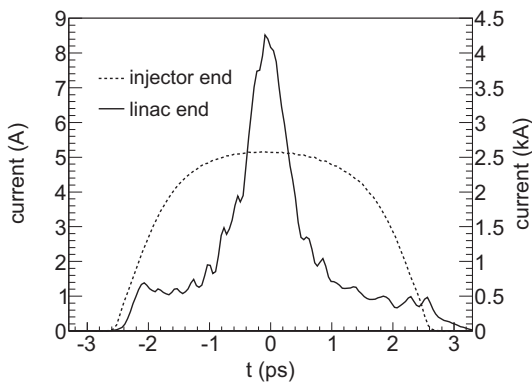


Figure 10: Current distribution of a 20 pC beam at the baseline injector end and at the linac end. The peak current is 4.2 kA at the linac end. The time axis for the linac end is multiplied by 100; the fwhm length is about 10 fs.

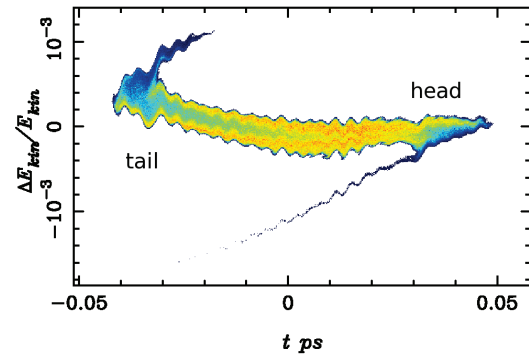


Figure 12: Time-energy phase space at the linac end for a 200 pC beam from the low emittance injector. A 100 kW heater laser power was applied to increase the uncorrelated energy spread to 10 keV at the injector end.

SUMMARY

shown in Fig. 12. A banana shape in time-energy phase space exists and further optimization is to be done to avoid this. The current profiles of a beam at the injector end and at the linac ends are compared in Fig. 13 for the 200 pC case from the low emittance injector. The normalized horizontal slice emittances are also compared in Fig. 14 at the injector and linac ends.

A preliminary study on microbunching instability using a model of the PAL-XFEL linac was carried out using the Elegant code. Strong instability of a bunch at the linac end could be reduced using a laser heater system. The electron bunch parameters at the linac end satisfy the requirements for SASE operation of PAL-XFEL.

Horizontal distortion of a bunch caused by CSR kick could be reduced arranging the last two chicanes to have

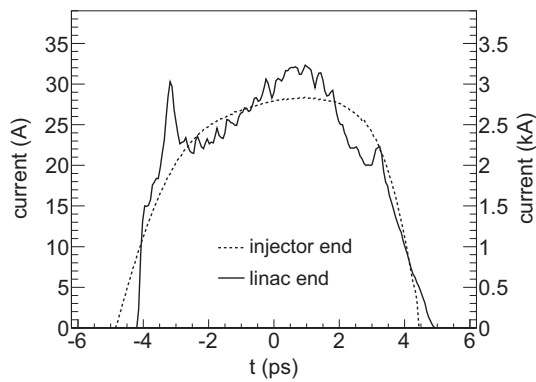


Figure 13: Current distribution of a 200 pC beam at the low emittance injector end and at the linac end. The peak current is 3.2 kA at the linac end. The time axis for the linac end is multiplied by 100.

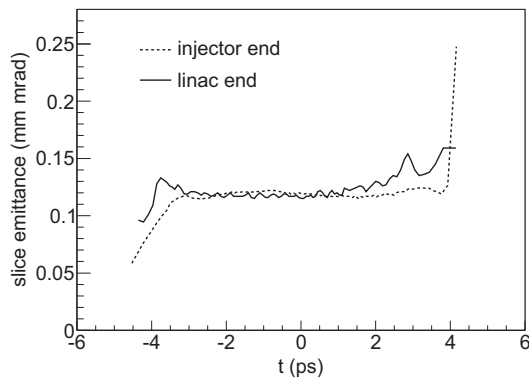


Figure 14: Normalized horizontal slice emittance of a 200 pC beam at the low emittance injector and linac ends. The time axis for the linac end is multiplied by 100.

horizontally opposite deflection direction.

Further optimization of the PAL-XFEL linac layout for better beam parameters is to be continued. More detailed study including 3D space charge effect and 3D CSR will be carried out.

REFERENCES

- [1] J.-H. Han, H.-S. Kang, I. S. Ko, IPAC2012, p. 1735.
- [2] H.S.Kang et al., these proceedings, TUPD34.
- [3] M. Borland, Elegant: A flexible sdds-compliant code for accelerator simulation, LS-287, Argonne National Laboratory (2000).
- [4] J.-H. Han et al., IPAC2012, p. 1732.
- [5] J.-H. Han et al., these proceedings, MOPD41.